JOC*Article*

Toward Self-Assembled Surface-Mounted Prismatic Altitudinal Rotors. A Test Case: Trigonal and Tetragonal Prisms

Douglas C. Caskey and Josef Michl*

Department of Chemistry and Biochemistry, University of Colorado, Boulder, Colorado 80309-0215

michl@eefus.colorado.edu

Received March 3, 2005

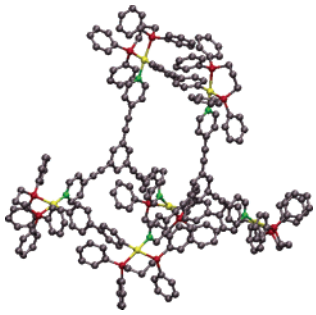

A self-assembly path toward prismatic molecular rotors based on transversely reactive terminally metalated molecular rods and pyridine-terminated star connectors has been extended. The concept has been tested on the assembly of trigonal and tetragonal prisms from the biphenyl rod, $[Ph_2P(CH_2)_3PPh_2]Pt^+$-C_6H_4-C_6H_4-$Pt^+[Ph_2P(CH_2)_3PPh_2]$, and the star-shaped connectors, 1,3,5-tris-(4-ethynylpyridyl)benzene and [tetrakis(4-pyridyl)cyclobutadiene]cyclopentadienylcobalt, respectively. The prisms have been fully characterized by NMR and MS, including diffusion-ordered NMR and collision-induced dissociation, and their chiral structures optimized by molecular mechanics are discussed.

For some time,[1] this laboratory has been developing a molecular assembly kit of rods[2] and star-shaped connectors[3−5] analogous to elements of the children's "Tinkertoy"[6] construction set. They have been used to assemble surface-mounted structures[7] including a molecular rotor whose dipolar rotator can be flipped by the electric field of an STM (scanning tunneling microscope) tip.[8]

Flow-Driven Altitudinal Rotors. We next wish to examine the possibility that surface-mounted altitudinal (axle parallel to surface) molecular rotors could be driven by fluid (gas or liquid) flow parallel to the surface. According to molecular dynamics calculations, chiral azimuthal (axle perpendicular to surface) rotors mounted on a grid can be driven with a flow of gas,[9] but such simulations have not yet been performed for altitudinal rotors. The altitudinal rotors would be half-buried in a self-assembled monolayer of a height that permits the flow to push only the rotator paddle that is most distant from the surface at any one moment. We expect that rotors carrying rotators with three or four large paddles would offer advantages, but unhindered rotation then requires that the rotor axle be located farther away from the surface than was the case in the first-generation surface-mounted altitudinal rotor.[8] It appears to us that large molecules consisting of edges of regular prisms,

(1) (a) Kaszynski, P.; Michl, J. *J. Am. Chem. Soc.* **1988**, *110*, 5225. (b) Michl, J.; Kaszynski, P.; Friedli, A. C.; Murthy, G. S.; Yang, H. C.; Robinson, R. E.; McMurdie, N. D.; Kim, T. In *Strain and Its Implications in Organic Chemistry*; de Meijere, A., Blechert, S., Eds.; NATO ASI Series, Vol. 273; Kluwer Academic Publishers: Dordrecht, The Netherlands, 1989; p 463. (c) Kaszynski, P.; Friedli, A. C.; Michl, J. *J. Am. Chem. Soc.* **1992**, *114*, 601.

(2) (a) Schwab, P. F. H.; Levin, M. D.; Michl, J. *Chem. Rev.* **1999**, *99*, 1863. (b) Schwab, P. F. H.; Smith, J. R.; Michl, J. *Chem. Rev.* **2005**, *105*, 1197.

(3) Schöberl, U.; Magnera, T. F.; Harrison, R. M.; Fleischer, F.; Pflug, J. L.; Schwab, P. F. H.; Meng, X.; Lipiak, D.; Noll, B. C.; Allured, V. S.; Rudalevige, T.; Lee, S.; Michl, J. *J. Am. Chem. Soc.* **1997**, *119*, 3907.

(4) Harrison, R. M.; Brotin, T.; Noll, B. C.; Michl, J. *Organometallics* **1997**, *16*, 3401.

(5) Schwab, F. H.; Noll, B. C.; Michl, J. *J. Org. Chem.* **2002**, *67*, 5476.

(6) Tinkertoy is a trademark of Playskool, Inc., Pawtucket, RI 02862 and designates a children's toy construction set consisting of straight wooden sticks and other simple elements insertable into spool-like connectors.

(7) Magnera, T. F.; Michl, J. *Proc. Natl. Acad. Sci. U.S.A.* **2002**, *99*, 4788.

(8) Zheng, X.; Mulcahy, M. E.; Horinek, D.; Galeotti, F.; Magnera, T. F.; Michl, J. *J. Am. Chem. Soc.* **2004**, *126*, 4060.

(9) Vacek, J.; Michl, J. *New J. Chem.* **1997**, *21,* 1259.

10.1021/jo050409c CCC: $30.25
Published on Web 06/09/2005

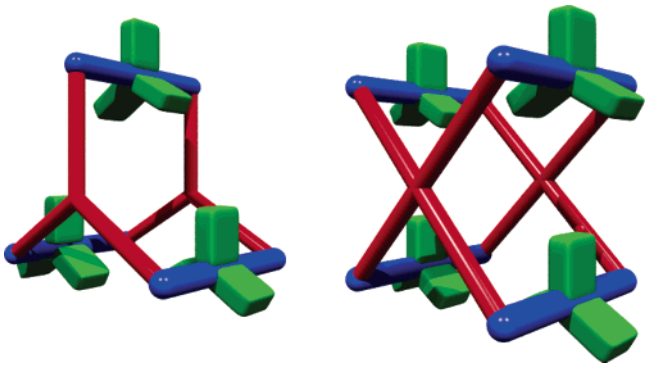

FIGURE 1. Prototypes of prismatic altitudinal rotors. The image of the rotor on the left has been reprinted with permission from *Chem. Rev.* **2005**, *105* (4), cover. Copyright 2005 American Chemical Society.

particularly trigonal and tetragonal, might be a suitable choice. Two edges of the prism would be adsorbed on the surface, and one or more other edges would represent axles carrying rotators to be driven by the flow. The prisms would be sturdiest if all edges were defined by molecular rods, but such structures are not represented in the literature to our knowledge. It appears easier and might be adequate to sacrifice some rigidity and to span polygonal faces in a face-directed manner and to define the remaining two edges of each rectangle with rods (Figure 1).

The logical way to synthesize large and relatively rigid prism skeletons of the type shown in Figure 1 is transition-metal-mediated, coordination-driven self-assembly,[10−12] already known to produce highly symmetric structures such as regular polygonal macrocycles and polyhedral boxes.[11,13] Assemblies of lower symmetry such as rectangular ("digonal"),[14−16] trigonal,[17] and tetragonal[18] prisms are less common and are typically composed of building blocks that span the faces of the product and leave the edges vacant.[19] Much of this self-assembly relies on rigid building blocks with fixed dihedral angles for the free valence of the reactive sites used in the assembly.

Prismatic Rotor Design. We have chosen to adopt parallel prism edges defined with linear building blocks designed to carry rotators and terminated with a metal atom whose active site is transversely directed. To our knowledge, 3-D prisms whose rectangular face edges are defined by roughly parallel rods and whose corners are represented with a metal atom have not been reported before.

As shown in Figure 1, we aim for right valence angles at the metal atoms in the corners, i.e., a cis relation between the bonds from the metal to the rod and to the arm of the trigonal or tetragonal connector. This can be assured by blocking the other two cis positions in a square planar metal complex with a bidentate ligand. The next issue is the relative orientation of the transverse reactive sites at the termini of the rod or of the connector. They could be rigidly fixed into syn parallel orientations, facilitating the desired self-assembly, or they could be free to rotate. Since we shall ultimately need an essentially free rotator in the center of the rod it would be complicated to fix the dihedral angle between the two transverse bonding directions at its termini. Fixing the dihedral angles at the three or four termini of the connector would introduce some synthetic complexity as well.

Not fixing the dihedral angles is a potentially serious disadvantage, because helicates, catenanes, rotaxanes, knots, and oligomers are then often formed preferentially in the absence of a template.[20] In fact, the initial syntheses of related organometallic rectangle[14] and trigonal prism[21] structures, in which the metal centers were located near the corners, were successful only after the dihedral angle was fixed. More recently, however, Stang and collaborators have reported other related structures such as 2-D macrocycles[22] and 3-D cages[23] using linear ligands with rotatable reactive sites. This offered hope that the synthetic challenge of fixing the dihedral angle between the reactive sites on a rod while maintaining free rotation for the rotator, or the dihedral angles between the reactive termini of a connector, could be avoided. We decided to test this synthetically simpler approach first.

To ensure that the metal atom can only connect two unlike building blocks during the self-assembly process, and not two like ones, we chose to have the metal atom covalently and permanently attached to a building block on one side, either the rod or the connector. To encourage flawless self-assembly, we still use a reversibly produced metal−ligand connection to the other side. Thus, two types of structures are possible: with the metal covalently attached as the terminus of the rod or as the terminus of the connector arm. The labile reversibly formed bond then needs to be produced in a direction transverse to the rod or to the connector arm, respectively. We have chosen to attach the metal atom covalently to the rod, since this allows us to use a supply of trigonal and tetragonal connectors with pyridine termini that are already available in our laboratory.[24] For

(10) (a) Baxter, P. N. W. In *Comprehensive Supramolecular Chemistry*; Lehn, J. M., Chair, E., Atwood, J. L., Davis, J. E. D., MacNichol, D. D., Vögtle, F., Eds.; Pergamon Press: Oxford, UK, 1996; Vol. 9, Chapter 5, p 165. (b) Lehn, J.-M.; Ball, P. *New Chem.* **2000**, 300. (c) Fujita, M. *Chem. Soc. Rev.* **1998**, *27*, 417. (d) Balzani, V.; Gomez-Lopez, M.; Stoddart, J. F. *Acc. Chem. Res.* **1998**, *31*, 405. (e) Cotton, F. A.; Lin, C.; Murillo, C. A. *Acc Chem. Res.* **2001**, *34*, 759.

(11) Leininger, S.; Olenyuk, B.; Stang, P. J. *Chem. Rev.* **2000**, *100*, 853.

(12) Caulder, D. L.; Raymond, K. N.; *Acc. Chem. Res.* **1999**, *32*, 975.

(13) Sweigers, G. F.; Malefetse, T. J. *Chem. Rev.* **2000**, *100*, 3483.

(14) Kuehl, C. J.; Huang, S. D.; Stang, P. J. *J. Am. Chem. Soc.* **2001**, *123*, 9634.

(15) Sommer, R. D.; Rheingold, A. L.; Goshe, A. J.; Bosnich, B. *J. Am. Chem. Soc.* **2001**, *123*, 3940.

(16) Caskey, D. C.; Shoemaker, R. K.; Michl, J. *Org. Lett.* **2004**, *6*, 2093.

(17) Kuehl, C. J.; Kryschenko, Y. K.; Radhakrishnan, U.; Seidel, S. R.; Huang, S. D.; Stang, P. J. *Proc. Natl. Acad. Sci. U.S.A.* **2002**, *99*, 4932.

(18) Yamanoi, Y.; Sakamoto, Y.; Kusukawa, T.; Fujita, M.; Sakamoto, S.; Yamaguchi, K. *J. Am. Chem. Soc.* **2001**, *123*, 980.

(19) Yamamoto, T.; Addicott, C.; Caskey, D. C.; Hawkridge, A. M.; Muddiman, D. C.; Shoemaker, R. K.; Kottas, G. S.; Horinek, D.; Michl, J.; Stang, P. J. Unpublished results, 2004.

(20) Fujita, M.; Ibukuro, F.; Seki, H.; Kamo, O.; Imanari, M.; Ogura, K. *J. Am. Chem. Soc.* **1998**, *120*, 611.

(21) Kuehl, C. J.; Yamamoto, T.; Seidel, S. R.; Stang, P. J. *Org. Lett.* **2002**, *4*, 913.

(22) Chi, K. W.; Addicott, C.; Arif, A. M.; Das, N.; Stang, P. J. *J. Org. Chem.* **2003**, *68*, 9798.

(23) Mukherjee, P. S.; Das, N.; Stang, P. J. *J. Org. Chem.* **2004**, *69*, 3526.

(24) Schwab, P. F. H.; Noll, B. C.; Michl, J. *J. Org. Chem.* **2002**, *67*, 5476.

SCHEME 1. Self-assembly of 4 and 5

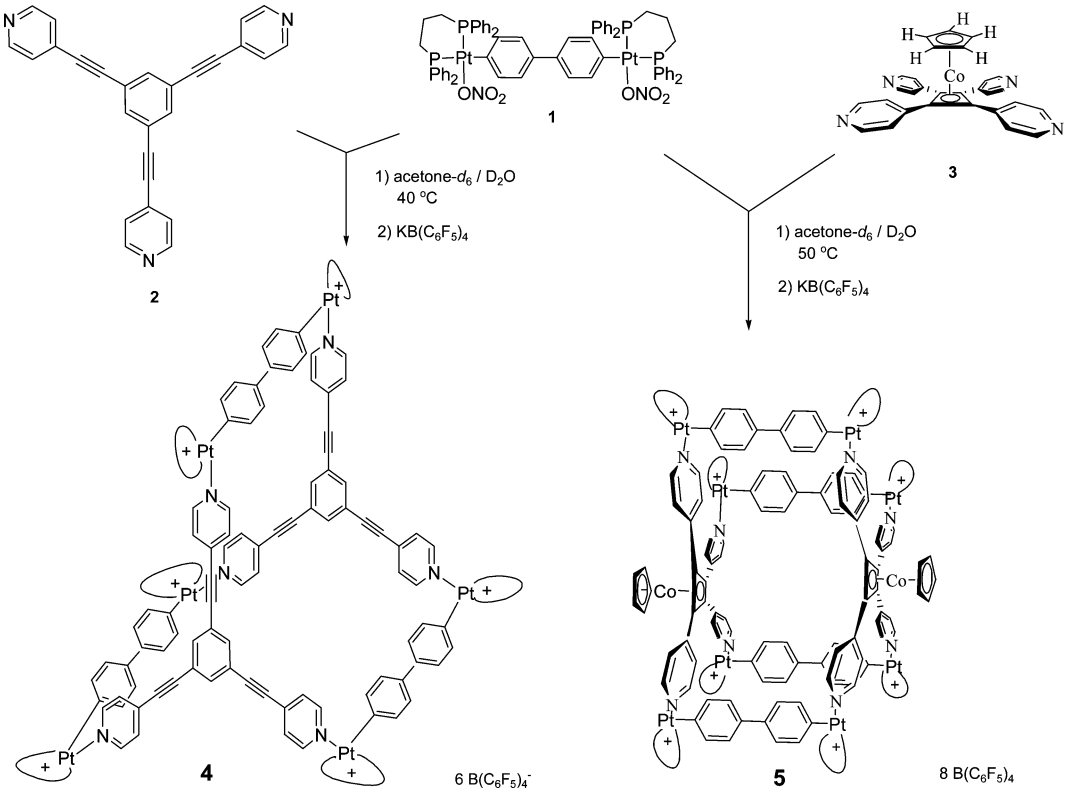

the initial testing of the synthetic concept, we have decided to use a simple rod without any rotators.

The above-described approach to supramolecular synthesis has already passed an initial test in which the rod **1** and a "two-armed star connector", 4,4′-bipyridyl, were found to form a rectangular "digonal prism" readily.[16] We now report the results of a more demanding test in which **1** is combined with the three- and four-armed star connectors, 1,3,5-tris(4-ethynylpyridyl)benzene **2** and [tetrakis(4-pyridyl)cyclobutadiene]cyclopentadienylcobalt **3**. Self-assembly is expected to yield the trigonal prism **4** and the tetragonal prism **5**, respectively.

Results

Synthesis. The general procedure for the assembly of **4** and **5** consisted of preparing a suspension of **1** and the appropriate ligand, **2** or **3**, in acetone-d_6/D_2O, which slowly dissolved upon heating. The products **4** and **5** were precipitated by addition of $KB(C_6F_5)_4$, chosen for the low nucleophilicity of its anion, which is expected to impart kinetic stability to the products (Scheme 1). We were unable to grow X-ray diffraction quality crystals of the products, but their composition, structure, and purity were determined beyond reasonable doubt by a combination of multinuclear and diffusion-ordered NMR, ESI-MS-CID, and elemental analysis.

Nuclear Magnetic Resonance. The NMR spectra of both **4** and **5** have been fully assigned and in each case fit the presence of a single type of square planar Pt atom carrying the 1,3-bis(diphenylphosphino)propane (dppp) ligand and two distinct aromatic rings in cis orientation. Signals of only one type of biphenyl rod and one type of connector arm terminating in pyridine are present, compatible with product structures consisting of bicyclic (**4**) or tricyclic (**5**) cages of alternating biphenyl moieties and star connectors linked via Pt^+(dppp) cations. Only one sharp signal is present for each ortho and meta ^1H and ^{13}C atom in each aromatic ring down to −90 °C, demonstrating the equivalence of the two termini of each rod, and the equivalence of all arms of the star connector. The absence of exo-endo differentiation of rod edges is attributed to rapid twisting equilibration. UFF[25] geometry optimization (Figure 2) showed that **5** can accommodate zero, one, or two Co(Cp) moieties inside the cage, but NOE contacts between the protons of the dppp phenyls and of the Cp rings demonstrate that in solution at least one of the −CoCp moieties is located outside the cage. From the equivalence of the Cp signals it follows that both lie outside.

The ^{195}Pt NMR spectra reveal a doublet of doublets for both **4** (J_{P-Pt} = 3619 and 1572 Hz) and **5** (J_{P-Pt} = 3602 and 1539 Hz), consistent with Pt satellites observed in the ^{31}P spectra. The $^{31}P\{^1H\}$ NMR spectrum of **5** reveals two doublets (J_{PP} = 25 Hz), one at 3.5 ppm, cis to pyridine (determined by NOE), with ^{195}Pt satellites (J_{PPt} = 1541 Hz), and another of equal intensity at −6.6 ppm, trans to pyridine (NOE), J_{PPt} = 3600 Hz. Similarly, the $^{31}P\{^1H\}$ NMR spectrum of **4** reveals two singlets, one at 3.4 ppm, cis to pyridine (NOE), with ^{195}Pt satellites (J_{PPt} = 1557 Hz), and another of equal intensity at −5.6 ppm, trans to pyridine (NOE), J_{PPt} = 3615 Hz. Chemical shifts and coupling constants of ^{195}Pt and ^{31}P are similar to those observed for the rectangle constructed with **1**.[16] The ^1H NMR spectrum shows a single set of α pyridine

(25) Rappe, A. K.; Casewitt, C. J.; Colwell, K. S.; Goddard, W. A., III; Skiff, W. M. *J. Am. Chem. Soc.* **1992**, *114*, 10024.

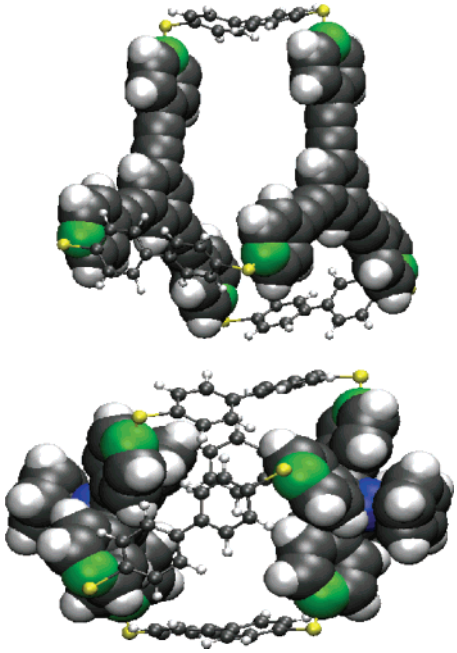

FIGURE 2. UFF[24]-optimized structure of molecular prisms **4** and **5**.

protons, at 8.5 ppm for **4** and at 8.4 ppm for **5**. The β pyridine protons of **4** produce a single set of signals at 7.1 ppm. The signals from the β protons of **5** are obscured under a set of signals from biphenyl at 7.9 ppm but have been revealed and assigned through 2-D correlation experiments. Also diagnostic is a single resonance from the protons of the central benzene ring of the star connectors in **4** at 7.5 ppm and a single resonance from the protons of the cyclopentadienyl (Cp) rings in **5** at 4.4 ppm. Compared to the free ligands **2** and **3**, the pyridyl signals shift upfield an average of 0.3 ppm for **4** and 0.5 ppm for **5**, respectively. This is attributed to shielding by the dppp phenyl rings (Figure 2), as has been reported for similar systems.[26] The ^{13}C NMR spectrum revealed C_i of biphenyl as a doublet of doublets in **4**, $J_{P-C} = 101$ and 7 Hz and **5**, $J_{P-C} = 104$ and 8 Hz. No coupling was observed to ^{195}Pt, probably because the ^{195}Pt satellites were below the noise level.

Assignments of signals were made through the use of gCOSY, gHSQC, and gHMBC experiments. A typical procedure is described for **4**. An HMBC experiment established one ^{1}H multiple-bond correlation to $^{13}C_i$ at 6.57 ppm, thus allowing us to assign $^1H_{m,biph}$. One single-bond ^{13}C correlation to $^1H_{m,biph}$ was observed at 123.5 ppm by HSQC, allowing assignment of $^{13}C_{m,biph}$. The $^1H_{m,biph}$ signal is correlated to only one ^{1}H signal at 6.99 ppm, allowing the assignment of $^1H_{o,biph}$. One single-bond ^{13}C correlation to $^1H_{o,biph}$ was observed by HSQC at 135.8 ppm. The $^1H_{o,biph}$ signal was correlated to both $^{13}C_{o,biph}$ and another quaternary carbon ($^{13}C_{p,biph}$), at 125.4 ppm. The $^{13}C_{p,biph}$ signal is not correlated to any other ^{1}H signals. Assignments of ^{1}H and ^{13}C spectra of the pyridyl star connectors of **4** and **5** were made similarly.

NOE has been used to examine group proximity. To eliminate the possible loss of NOE correlations due to rotational correlation times approaching $1/\omega_0$, the rotating frame ROESY method was used. NOE signals were observed from $^1H_{\alpha,pyr}$ to $^1H_{\beta,pyr}$, $^1H_{o,biph}$, and $^1H_{o,ph}$ for **4** and **5**, as well as from $^1H_{Cp}$ to $^1H_{\beta,pyr}$ and $^1H_{m,ph}$. These results support the expected cis arrangement around the metal center of biphenyl with **2** and **3** in **4** and **5**, respectively, and leave no doubt that the products have a molecular structure consisting of alternating biphenyl and star-shaped connector units.

TABLE 1. Radii of Prisms 4 and 5

compd	D[a]	R from D[b]	R from UFF[c]
digonal prism[16]	5.18	10.2	11.4
trigonal prism **4**	2.17	17.6	15.2
tetragonal prism **5**	4.04	13.1	12.7

[a] Diffusion coefficient in units of 10^{-10} m^2 s^{-1}, obtained from DOSY measurements in CD_2Cl_2 at 298 K. [b] Radius in Å, calculated from the Stokes−Einstein equation. [c] Approximate distance in Å from the prism center to the central $-CH_2-$ moiety of the dppp ligand in the UFF[25]-optimized geometry. An approximate value of each "experimental" radius R was calculated from the diffusion coefficient using the Stokes−Einstein equation, $D = k_BT/6\pi R\eta$, where D is the diffusion coefficient, k_B is the Boltzmann constant, T is the absolute temperature, and η is the viscosity of methylene chloride (0.0041 g s^{-1} cm^{-1}). The distance from prism center to the central $-CH_2-$ moiety of the dppp ligand was used as an approximate measure of the radius R of the smallest sphere required to enclose a prism. The sizes found experimentally agree roughly with calculations and support the postulated formation of discrete prisms composed of two star-shaped connectors and three organometallic rods for **4** and two connectors and four rods for **5**.

In synthesis by self-assembly there is always danger of forming larger aggregates than intended. We have therefore examined the size of **4** and **5** by diffusion-ordered NMR (DOSY) with ^{1}H detection. The observed values were compared to that found for the rectangle previously formed from **1** and 4,4′-bipyridyl[16] (Table 1).

Mass Spectrometry. An independent confirmation of the structural assignment of **4** and **5** was obtained from electrospray ionization mass spectra. The spectrum of **4** showed $[M - B(C_6H_5)_4]^+$, $[M - 2B(C_6H_5)_4]^{2+}$, $[M - 3B(C_6H_5)_4]^{3+}$, and $[M - 4B(C_6H_5)_4]^{4+}$ peaks at the values of *m/z* 8259.2, 3789.7, 2300.2, and 1555.6, respectively, expected for **4**, with the anticipated isotropic distribution patterns. $[M - nB(C_6H_5)_4]^{n+}$ peaks were observed with $n > 4$. Similarly, the spectrum of **5** showed $[M - B(C_6H_5)_4]^+$, $[M - 2B(C_6H_5)_4]^{2+}$, and $[M - 3B(C_6H_5)_4]^{3+}$ peaks at the values of *m/z* 11191.1, 5256.1, and 3277.5, respectively, expected for **5**, with the anticipated isotropic distribution patterns (Figure 3). $[M - nB(C_6H_5)_4]^{n+}$ peaks were observed with $n > 3$. Several fragment peaks in the spectra of **4** and **5** correspond to the cleavage of two Pt−N bonds and to a loss of one organometallic rod. For **4** they occur at *m/z* 5534.3 with a spacing of $\Delta m = 1$ amu and at *m/z* 2427.7 with a spacing of $\Delta m = 0.5$ amu. For **5**, they are at *m/z* 3893.5 with a spacing of $\Delta m = 1$ amu, 2369.3 with a spacing of $\Delta m = 1/2$ amu, and *m/z* 1607.2 with a spacing of $\Delta m = 1/3$ amu. For **4** there also is a peak which corresponds to the loss of two organometallic rods at *m/z* 2808.3, but its resolution is insufficient for an independent charge state determination.

Collision-induced dissociation (CID) on the *m/z* 2300 ion $[M - 3B(C_6H_5)_4]^{3+}$ confirmed the structure **4** (Figure 4). The peak at *m/z* 2427.7, with a spacing of $\Delta m = 0.5$ amu, corresponds to the cleavage of two Pt−N bonds and the loss of one organometallic rod, the peak at *m/z* 2808.3,

(26) Stang, P. J.; Danh, C. H. *J. Am. Chem. Soc.* **1994**, *116*, 4981.

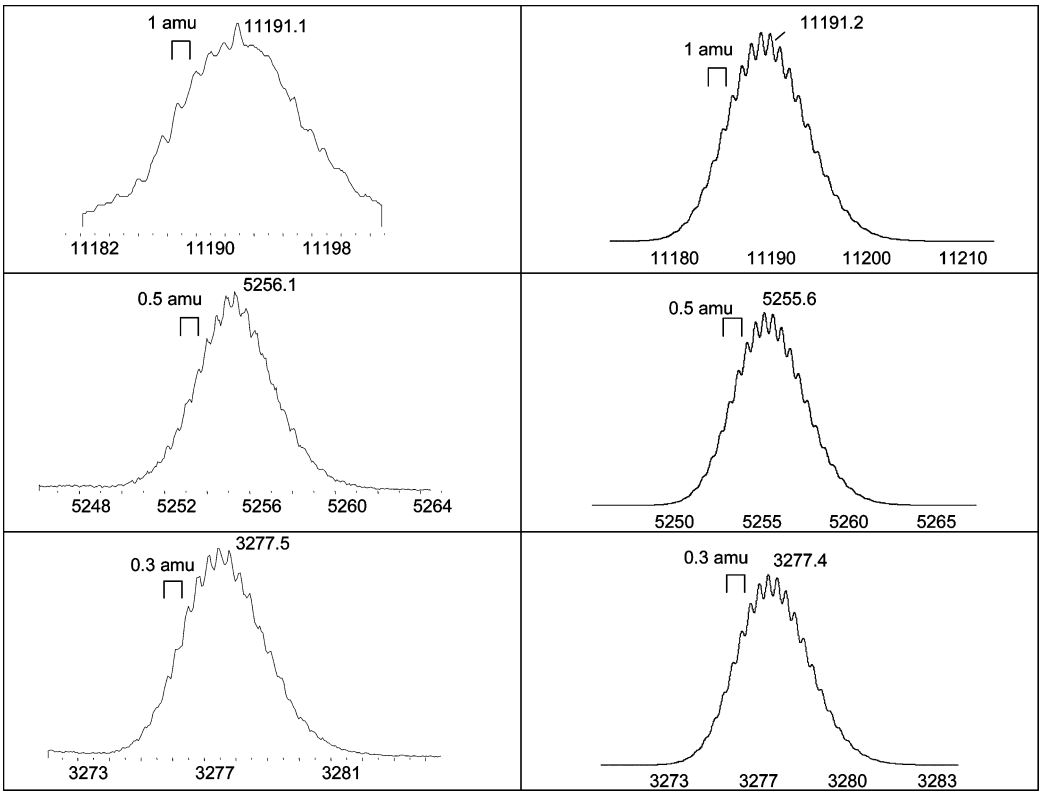

FIGURE 3. Observed (left) and calculated (right) isotopic distribution patterns of **5**: M − 1B(C_6F_5)$_4$, M − 2B(C_6F_5)$_4$, and M − 3B(C_6F_5)$_4$.

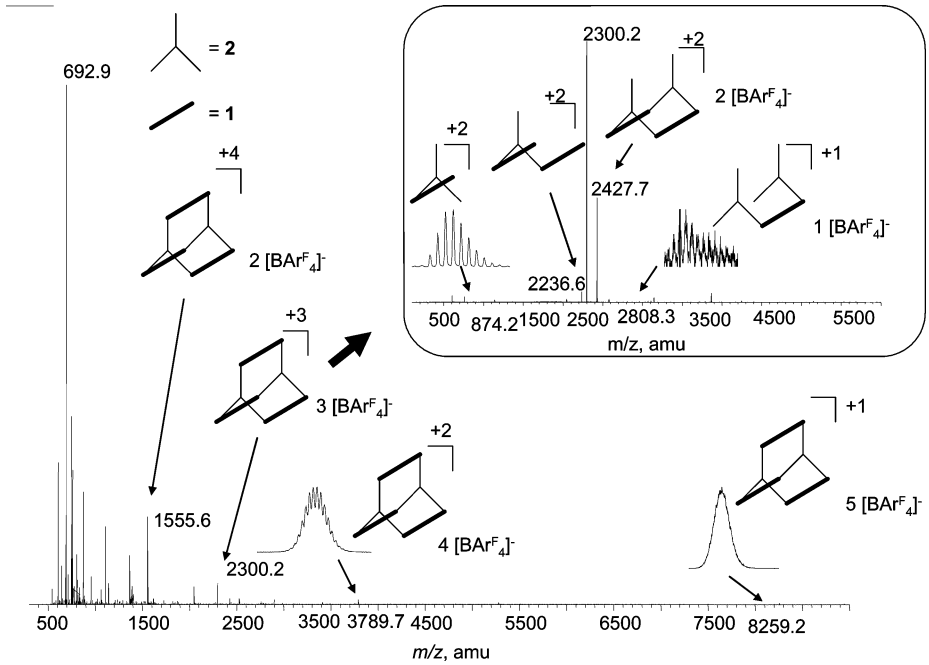

FIGURE 4. ESI-MS of **4** and CID of peak at *m/z* 2300.

with a spacing of Δm = 1 amu, corresponds to loss of two rods, a peak at *m/z* 2236.6, with a spacing of Δm = 0.5 amu, corresponds to the loss of one rod and one connector, and the peak at *m/z* 874.2, with a spacing of Δm = 0.5 amu, corresponds to one rod and one connector. CID of **5** resulted in only small fragments revealing little structural information about **5**.

Molecular Mechanics Calculations. The results of a UFF optimization of **4** and **5** are shown in Figure 2, and the most important geometrical parameters are collected in Table 2 and defined in Figure 5. There is nothing remarkable about the computed structures of the individual building blocks, such as the 26−37° twist about the central bond of the biphenyl units, and it is

TABLE 2. UFF-Optimized Structures of 4 and *5* (cf. Figure 5)[a]

compd	α[b]	β[c]	γ_{ph}[d]	γ_{py}[e]	δ[f]	E[g]
4 PPP	+15	+36, +35, +32	+72, +78, +74, +78, +73, +76	+72, +85, +76, +76, +76, +84	85	0
4 PPM	+11	+32, +34, −27	+61, +85, +77, +84, −73, −74	+76, +73, +76, +77, −88, −77	76	2
5 PPPP	+29	+26, +25, +25, +26	+70, +68, +60, +70, +69, +82, +81, +55	+74, +70, +72, +64, +71, +66, +68, +68	70	0
5 PPPM	+31	+22, +28, +27, −18	+69,+71,+62,+78, +85,+59,−82,−86	+75 ,+67, +70, +89, +80, +68, −75, −71	59	6
5 PPMM	+39	+27, +18, −27, −41	+64,+66,+72,+53, −88, −91, −72, −89	+72, +72, +90, +72, −77, −78, −88, −84	51	10

[a] The sign of the reported angles indicates the sense of the twist. The angles γ_{ph} and γ_{py} are given in pairs for the two ends of a prism edge, with edges in the sequence shown under the compound label. [b] Prism twist angle. [c] Biphenyl twist angle. [d] Angle between the benzene ring and the N−Pt−C coordination plane. [e] Angle between the pyridine ring and the C−Pt−N coordination plane. [f] Average angle between the planes of the central rings of the star-shaped connectors and the Pt−Pt prism edges of the cage. [g] Relative energy in kcal/mol.

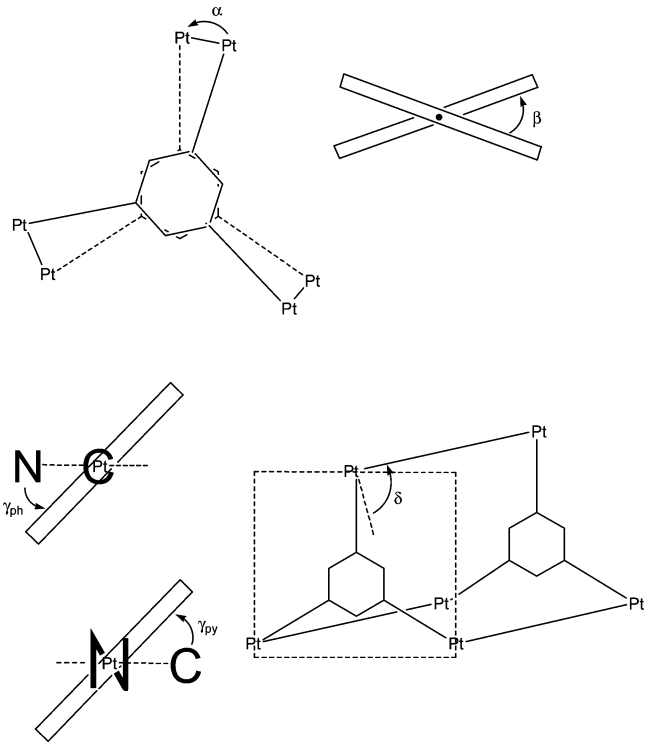

FIGURE 5. Definition of angles used in Table 2.

their relative orientation and chirality that are of interest. Two low-energy diastereomers of **4** have been found (Table 2), differing in the relative sense of the helical twist in the three biphenyls. In one pair of enantiomers, all three are twisted alike (PPP, shown in Figure 2, or MMM), and in the other, only two are (PPM or MMP). The former is calculated to be 1.5 kcal/mol more stable (i.e., of equal stability within the error of the method), and the interconversion of the diastereomers is undoubtedly very facile. In both diastereomers, the arms of the two trigonal connectors are nearly exactly eclipsed, and the easy interconversion makes the effective symmetry D_{3h} at all but the very lowest temperatures.

The situation is different with **5** (Table 2). In accord with the crystal structure of **3**,[4] each pyridine ring on the crowded cyclobutadienes is calculated to be twisted out of the cyclobutadiene plane in the same sense by ~38° and each square face of the prism is therefore chiral, P (shown in Figure 2) or M. The sense of this twist is communicated to the biphenyl ring that is also attached to the Pt atom. Both this benzene ring and the pyridine ring of the other ligand on the same Pt atom need to be twisted in the same sense relative to the C−Pt−N coordination plane (the twist angles γ_{ph} and γ_{py} have the same sign, cf. Table 2). When the handedness of both square connectors is the same, say P, it accommodates the equal sense (P) of the natural twist of the four biphenyl units much better than the opposite sense (M).

Steric interactions are minimized when the two square faces assume a mutual twist α of about ±30°, causing the system to be closer to a tetragonal antiprism (α = ±45°) than a tetragonal prism (α = 0°). The optimal conformation of **5** thus exists as a pair of enantiomers, PPPP and MMMM. We have also calculated two of the other conformers, in which one or two of the biphenyl rods are twisted in the sense opposite to the chiral faces, but their energies are higher (Table 2).

Discussion

The spectral results leave no doubt in our minds that the connectivity of the self-assembled products of **4** and **5** is as shown in Scheme 1. In the absence of X-ray diffraction structural data, however, it is not obvious that the stereochemical details of the structure are as hoped for and as shown in Figure 1. Specifically, it has not been shown that the arms of the two connectors are eclipsed as shown there, and that the three edges of the trigonal prism **4** and the four edges of the tetragonal prism **5** are parallel to each other and to the line connecting the centers of the connectors, and perpendicular to the planes of the connectors. This is important for our intended applications. If the connector arms are not eclipsed but rotated toward a staggered (antiprism) geometry, the opposite "prism" edges will no longer be parallel, making it more difficult for one of the prism faces to bind to a flat surface. Associated with this concern is the issue of the chirality of the rods, the connectors, and of the overall prismatic structure. The low-temperature NMR results demonstrate that the interconversion of possibly present stereoisomers is rapid, but their instantaneous 3-D structure nevertheless remains interesting, although not particularly relevant for our intended application.

At present, the molecular mechanics optimized geometries shown in Figure 2 are the only source of information on the detailed stereochemistry of **4** and **5**. The accuracy of the UFF force field is low. However, it is the best we can currently use, and its use appears reasonable

since the steric preferences are likely to be largely dictated by steric repulsions, which will be rendered qualitatively correctly.

The conclusion from Figure 2 is that the trigonal prism **4** is far closer to the ideal structure shown in Figure 1 than its tetragonal counterpart **5** and that its symmetry is close to D_{3h}. The difference between having three versus four edges is probably not instrinsic. Rather, the twist imposed on the pyridine rings of **5** by their crowding around the central cyclobutadiene rings is likely to be the culprit that makes **5** closer to being an antiprism than a prism. The problem could most likely be cured by the insertion of an acetylene or phenylacetylene unit between the four-membered ring and each of its four substituents, and such a tetragonal connector has been synthesized.[19] However, for the moment, it seems best to concentrate our future efforts on trigonal connectors based on 1,3,5-trisubstituted benzenes.

Conclusions

The evidence that **4** and **5** have been assembled is overwhelming. This result bodes well for the use of the same self-assembly method for the preparation of prismatic altitudinal rotors from rotator carrying rods terminated in metal atoms with a transversely directed active site, combined with pyridine-terminated star shaped connectors such as those that we have already synthesized. The logical next step thus would be the preparation of a trigonal prismatic rotor with actual rotators installed. However, even if this succeeds, important issues will remain to be addressed: kinetic stability of these prismatic rotors, their attachment to a surface, their potentially insufficient rigidity, and their undesirable net charge.

Finally, we believe that the concept of face-dictated chirality communicated from one face to another is of general interest and address the issue in more detail elsewhere.[19]

Supporting Information Available: Experimental procedures and characterization data. This material is available free of charge via the Internet at http://pubs.acs.org.

JO050409C